Astron. Astrophys. 360, 656–662 (2000)

ASTRONOMY AND ASTROPHYSICS

Ortho to para conversion of H_2 on interstellar grains

J. Le Bourlot

DAEC, Observatoire de Paris and Université Paris 7, UFR de Physique

Received 28 April 2000 / Accepted 15 June 2000

Abstract. Fast conversion of ortho-H_2 to para-H_2 can occur (and has been observed in the laboratory) on the surface of non magnetic, non metallic grains. In a PDR, the fraction of H_2 converted depends on the ratio of the characteristic time of conversion (of the order of 1 minute) to the residence time of physisorbed H_2. This later time is itself an exponentially varying function of the grain temperature and of the adsorption binding energy of H_2. Conversion is very efficient in cool PDRs if the dust temperature is below a critical temperature that we determine, and leads to a much reduced ortho to para ratio of H_2 in the gas phase. Emission lines within para levels of H_2 are significantly enhanced.

Key words: molecular processes – ISM: molecules – ISM: abundances – ISM: dust, extinction

1. Introduction

Due to the nuclear spin of its constituent atoms, H_2 exists in two modifications: para-H_2 with even J rotational numbers, and ortho-H_2 with odd J rotational numbers in its lowest electronic state. Conversion from one modification to the other requires a nuclear spin flip and is therefore forbidden for an isolated molecule. To date, the only mechanisms considered for connecting the two modifications within interstellar clouds have been gas phase reactions with H, H^+or H_3^+ which involve an exchange of a proton. Those reactions are slow in moderately bright PDRs, leading to a relaxation time for the ortho to para ratio (thereafter O/P ratio) typically much longer than the thermalization time within each modification. General references and a study of the O/P ratio in shocks can be found in Wilgenbus et al. (2000).

The fact that a nuclear spin flip without exchange of a proton requires a magnetic interaction leads to the common belief that it does not occur under interstellar conditions. Although spin conversion of molecules adsorbed on grains is mentioned in Tielens & Allamendola (1987), it has usually been neglected.

It is also well known that, in the molecular part of PDRs, collisions of H_2 with grains is by far the dominant gas-grain interaction, but the fate of those interacting H_2 molecules have been seldom considered, probably through the belief that rapid evaporation prevents any significant physical process to occur. Exceptions are the works of Sandford & Allamandola (1993), Dissly et al. (1994) and Buch & Devlin (1994) on the incorporation of H_2 into H_2O ices, but these authors did not consider the O/P ratio.

However, the physics of H_2 adsorbed on a surface has been the subject of considerable work within the condensed matter physics community, and, to my knowledge, most astrophysicists are not yet aware of some very significant results:

- First of all, conversion of ortho to para H_2 adsorbed on a cold (10 K) surface has been observed in the laboratory on non magnetic surfaces, both non-metallic (graphite) (Palmer & Willis (1987)) and metallic (Ag, Cu) (Ilisca (1991b)).
- Second, that conversion can be fast: in less than one minute there is only para-H_2 left (Palmer & Willis (1987)).
- Third, theoretical mechanisms that explain both how that conversion occurs and why it is so efficient have been proposed (e.g. Ilisca (1992), Ilisca (1991a) and Ilisca (1991b)).

All mechanisms involve the interaction of an adsorbed H_2 with an electron of the substrate leading to a transfer of angular momentum to the electron. The induced magnetic dipole may then interact with the nuclear spin and result in a change of modification. On graphite, the process is believed to occur with unpaired electrons at point defects in the crystalline structure.

Thus, there is no reason why the same transition could not occur within an interstellar cloud. The complete mechanism can be split into four steps:

- Collision of an H_2 molecule in the gas phase with a grain leads to an adsorbed (physisorbed) H_2. The sticking coefficient should be close to unity.
- The adsorbed molecule thermalizes at the grain temperature in a time scale of the order of the vibration time scale (10^{-13} s). Most physisorbed H_2 molecules are therefore in the lowest $(v, J) = (0, 0)$ and $(0, 1)$ rovibrational states.
- Conversion of ortho molecules occurs with a typical time scale $\tau_{\rm c}$ of one minute.
- Evaporation removes H_2 from the surface. The residence time $k_{\rm ev}^{-1}$ depends on the grain temperature $T_{\rm d}$ and the adsorption binding energy $T_{\rm ad}$.

Send offprint requests to: J. Le Bourlot
Correspondence to: Jacques.Lebourlot@obspm.fr

The fraction of H_2 converted is proportional to $\exp(-\tau_c\, k_{ev})$. In the following, we show that this process may be very efficient in regions where the grains are not too hot.

This paper is divided into three parts. In the first, the relevant parameters are reviewed and reasonable ranges of variation are estimated for the lesser known ones. In the second, the influence of that conversion mechanism on various steady state models of PDR is discussed. In the third part, comparisons with selected observations are made.

2. Physical parameters

Basics of interstellar dust structure and processes are taken from Tielens & Allamendola (1987) when no other reference is given.

2.1. Sticking coefficient

The sticking coefficient of H_2 on cold dust should be close to 1. That value is adopted and not varied in the following, since a value of 0.3 would not qualitatively change the results.

2.2. Binding energy

The binding energy of physisorbed H_2 molecule varies between $T_{ad} = 800\,K$ on a bare grain (Tielens & Allamendola (1987)) and only a few hundred K if an ice mantle has grown. Sandford & Allamandola (1993) derive a binding energy of $T_{ad} = 555\,K$ on $H_2O : CH_3OH$ ices from laboratory experiments and Katz et al. (1999) derive a binding energy of $T_{ad} = 541\,K$ on amorphous carbon. The binding energy of H_2 on a H_2 layer should be as low as $100\,K$, which prevents a large depletion of molecular hydrogen from the gas phase.

The full range from $T_{ad} = 100\,K$ to $T_{ad} = 1000\,K$ has been explored, but no variation as a function of A_v has been allowed yet. Since the grain surface state changes from the edge to the core of the cloud, we plan to include a depth dependant binding energy in a near future.

2.3. Conversion time scale

Little can be said on the conversion time scale else than it may be fast. From Palmer & Willis (1987), we deduce that it is smaller than $\tau_c = 60.0\,s$ on graphite at $10\,K$. That value is used in the following and has not been varied. It may also depend on the grain temperature in an unknown way, but this has not (yet?) been considered. In Sect. 2.5 we show that a variation of this time scale by an order of magnitude would not change qualitatively the results.

2.4. Grain temperature

The dust temperature T_d as a function of depth into the cloud is computed from Burton et al. (1990) and Hollenbach et al. (1991). Using their notation (Hollenbach et al. (1991), Eq. (5)), the dust temperature T_d in the outer layers of the cloud (where heating of dust results mainly from absorption of U.V. radiation) is:

$$T_d = \left(8.9\,10^{-11}\,\nu_0\,G_0\,\exp(-1.8\,A_v)\right)^{0.2} \quad (1)$$

Where ν_0 is a cut-off frequency which they estimate to be $\nu_0 = 3\,10^{15}\,s^{-1}$, and G_0 the radiation field strength in "Habing" units. In the following computations, we have used their full formula to derive the dust temperature as a function of A_v.

Recent I.R. observations (e.g. Laureijs (1999)) suggest that T_d could be significantly smaller than what Eq. 1 gives, maybe by as large as a factor of 2. The consequences of this possibility are explored in Sect. 4.

2.5. Conversion efficiency

The fraction of ortho-H_2 converted to para-H_2 depends on the residence time of H_2 on the grain. Here we derive analytical results valid if desorption is dominated by evaporation. Evaporation from grains proceeds at a rate (Tielens & Allamendola (1987), Eqs. (4) and (6) p. 432):

$$\begin{aligned} k_{ev}(T_{ad}, T_d) &= \tfrac{1}{\pi\, d_s}\sqrt{\tfrac{2\,k\,T_{ad}}{2\,m_H}}\exp\left(-\tfrac{T_{ad}}{T_d}\right) \\ &= \tau_v\,\sqrt{T_{ad}}\exp\left(-\tfrac{T_{ad}}{T_d}\right) \end{aligned}$$

where d_s is the mean distance between adsorption sites on the grain surface. We use $d_s = 2.6\,\text{Å}$. Numerically, this leads to $\tau_v = 1.1\,10^{11}\ s^{-1}K^{-1/2}$.

If conversion is described by a characteristic time τ_c, the fraction of H_2 molecules that undergoes a transition varies exponentially with the ratio of the conversion time τ_c to the residence time k_{ev}^{-1}. This leads to an efficiency:

$$\begin{aligned} \eta_c(T_{ad}, T_d) &= \exp(-\tau_c\, k_{ev}) \\ &= \exp\left(-\tau_c\,\tau_v\,\sqrt{T_{ad}}\,\exp\left(-\tfrac{T_{ad}}{T_d}\right)\right) \end{aligned}$$

This double exponential leads to a sharp transition in the (T_{ad}, T_d) plane between a region where $\eta_c = 0$ (high dust temperature, low binding energy) and a region where $\eta_c = 1$. The frontier can be determined analytically by computing where the second derivative of η_c is zero. One finds that the first derivative with respect to T_{ad} is proportional to the product $\eta_c \cdot k_{ev}$ (up to a slowly varying term), so that $\frac{\partial^2 \eta_c}{\partial T_{ad}^2} \propto (1 - \tau_c\, k_{ev})$. Thus we find a critical dust temperature for the ortho to para transition:

$$T_d^{crit}(T_{ad}) = \frac{2\,T_{ad}}{\ln(\tau_c^2\,\tau_v^2\,T_{ad})} \quad (2)$$

The resulting critical curve is displayed on Fig. 1. One can see that it is close to a straight line, although there is a small logarithmic correction. The fact that free parameters appear only within the $\ln()$ function renders it quite insensitive to uncertainties in the parameters: at $T_{ad} = 500\,K$, a variation by a factor of 10 of the factor $\tau_v^2\tau_c^2$ leads to only a 4% variation of T_d^{crit}.

Eqs. 1 and 2 may be combined to determine a critical A_v where conversion becomes effective (i.e. where T_d falls below

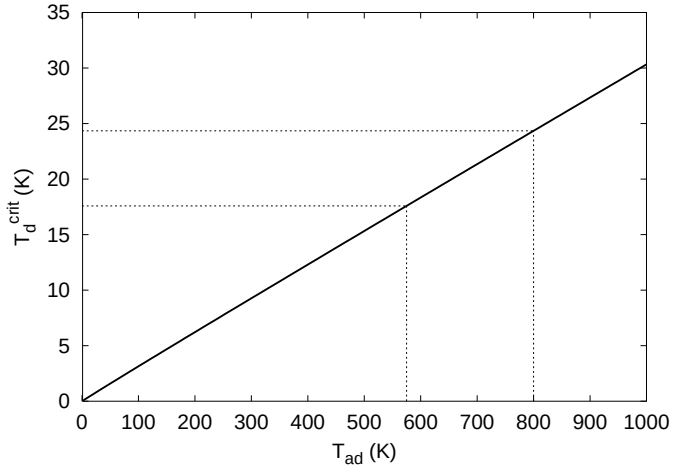

Fig. 1. Critical dust temperature as a function of H_2 binding energy for $\tau_c = 60\,s$ and $\tau_v = 1.1\,10^{11}\,s^{-1}K^{-1/2}$.

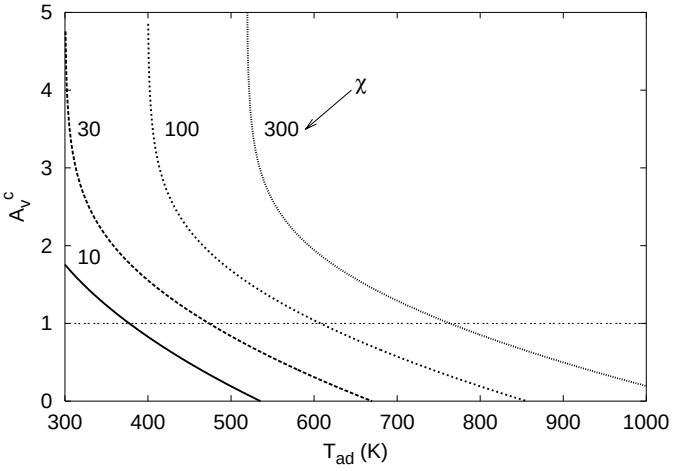

Fig. 2. Critical A_v as a function of T_{ad} for different radiation fields (labels are scaling factors of a "Mathis" radiation field) using T_d from Hollenbach et al. (1991) (full expression).

T_d^{crit}). This is displayed on Fig. 2 for different radiation fields (in units of the standard ISRF of Mathis[1]).

2.6. Other desorption mechanisms

The validity of Eq. 2 depends on the fact that desorption proceeds through evaporation. Alternative mechanisms are photo-desorption (either with incident U.V. photons or internally produced secondary photons) or grain collisions. These two processes have been included in the model and the computed residence time is

$$\tau_{res} = \frac{[H_2(ad)]}{\left.\frac{d[H_2(ad)]}{dt}\right|_{desorb}}$$

We have checked that $\tau_{res} = k_{ev}^{-1}$ in the region where H_2 is hot enough to emit vibrational lines. Photo-desorption becomes the dominant mechanism deeper into the cloud where grains are too cold to lead to a significant evaporation rate. Desorption is then dominated by photo processes involving internally produced secondary photons. However the point where η_c becomes significant is controlled by evaporation in all the cases we have checked: the worst case (high U.V. flux and reduced grain temperature) is displayed on Fig. 3. The corresponding model is described in Sect. 4.

[1] Note that the Habing flux is $1.6\,10^{-3}\,erg\,cm^{-2}s^{-1}$ at 1000Å. The resulting conversion between G_0 of Eq. 1 and χ is: $\chi = 1.31\,G_0$.

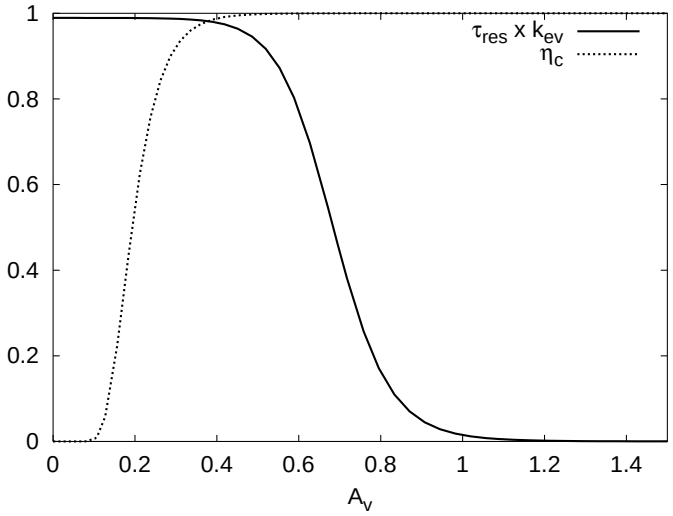

Fig. 3. Conversion efficiency (η_c) and ratio of residence time (τ_{res}) to evaporation time (k_{ev}^{-1}) for the last model of Sect. 4 ($\chi = 300, T_d \times 0.7$)

3. Models

The reference model has a constant density of $n_H = 10^4\,cm^{-3}$, exposed to a radiation field enhanced by a factor $\chi = 10$ above the standard Mathis field, and a cosmic ray ionisation rate of $5.0\,10^{-17}\,s^{-1}$. Abundances are those of the ζ Oph cloud, although those values have no influence on the excitation of H_2. H_2 is formed on grains with an initial O/P ratio of 3; conversion by collision with H, H^+ and H_3^+ is always included and dissociative recombination of H_3^+ gives H_2 with an O/P ratio of 2. Detailed balance of H_2 rovibrational levels is computed at each point into the cloud. We use the new collisional cross sections with H, He and H_2 from D. Flower and coworkers (see the references in Le Bourlot (2000)).

The grain size distribution follows a power law with an index of -3.5, with radii ranging from $3\,10^{-7}$ to $3\,10^{-5}\,cm$. All processes concerning grains, including adsorption and evaporation, are described in Le Bourlot et al. (1995). Desorption through grain-grain collisions and photons interactions are included. The dust temperature is not allowed to fall below $15\,K$, although this is somewhat arbitrary.

H_2 abundance and gas and grains temperature as a function of depth into the cloud are exhibited in Fig. 4 and 5 for $\chi = 10$ and $\chi = 100$. Most H_2 line emission arises from the outer region where H_2 has formed and the gas is still hot enough, that is between $A_v = 10^{-4}$ and $A_v = 1$ here. This is the region of interest which is discussed below.

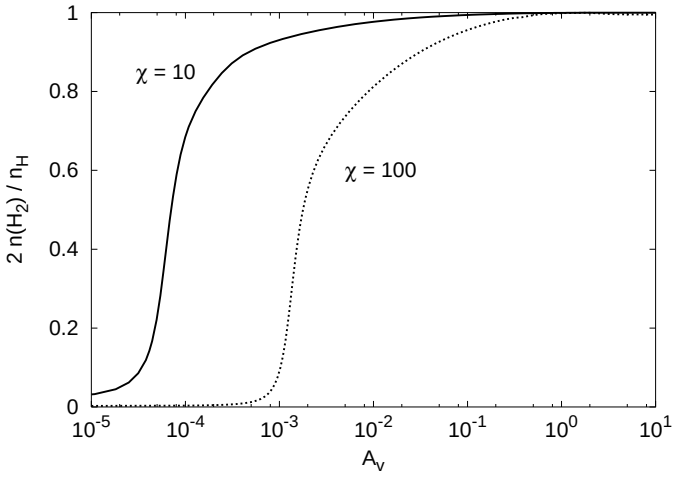

Fig. 4. Relative abundance of H_2

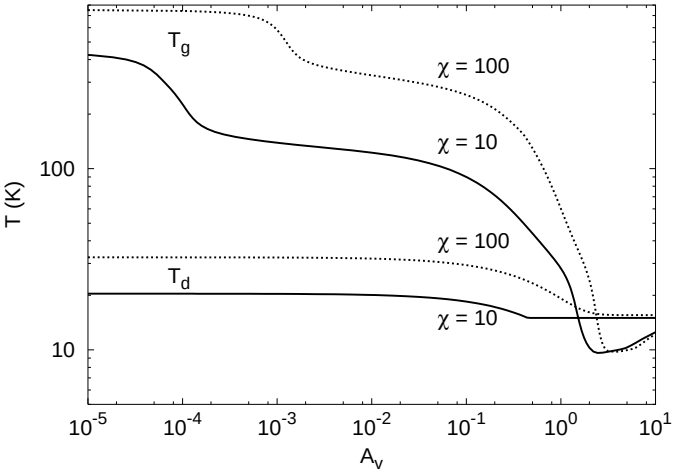

Fig. 5. Gas and grain temperature

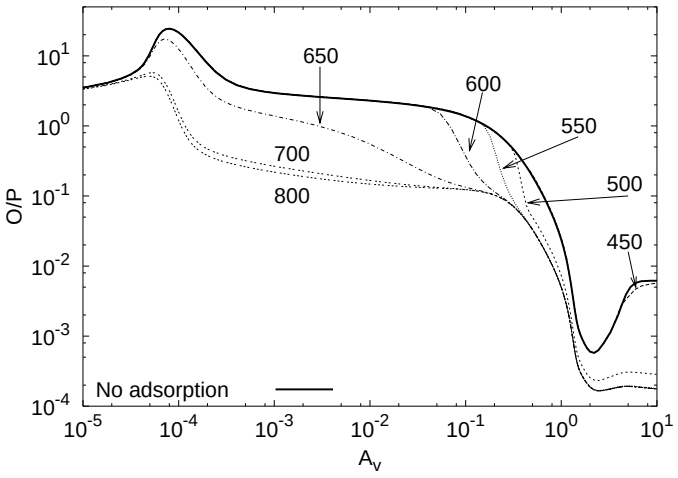

Fig. 6. Local O/P ratio for different H_2 binding energies (450, 500, 550, 600, 650, 700 and 800 K). $\chi = 10$, labels are $T_{\rm ad}$ in K. The "bump" at low $A_{\rm v}$ comes from a slightly more efficient self-shielding of ortho-H_2 leading to a $\rm H/o-H_2$ transition closer to the edge of the cloud (see Le Bourlot (2000)), The high $A_{\rm v}$ asymptotic value is dominated by recycling of H_2 through H_3^+ recombination (see Le Bourlot (1991)).

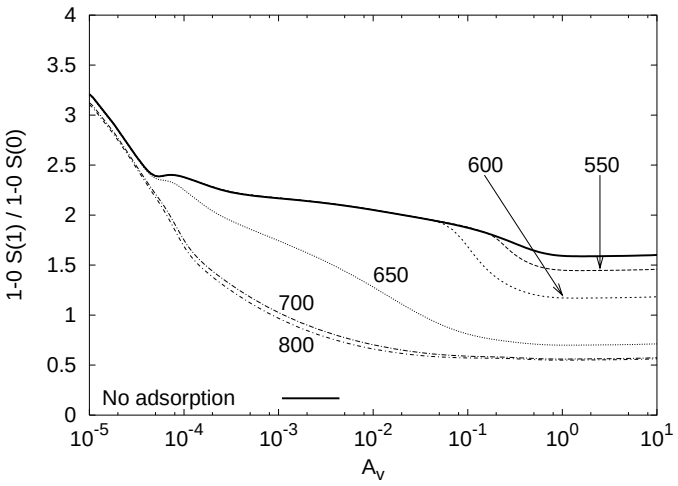

Fig. 7. Integrated (from the surface to $A_{\rm v}$) intensity ratios for the same binding energies as in Fig. 6, except $T_{\rm ad} = 450$ and 500 K which are too close to the "No adsorption" case.

3.1. Influence of the binding energy

The binding energy of an adsorbed H_2 molecule on a grain is varied between $T_{\rm ad} = 450$ K and $T_{\rm ad} = 800$ K. Outside that range, we have checked that the curves fall onto one another. Fig. 6 shows the resulting local O/P ratio.

It is seen that in that the total O/P ratio falls from 3 to 0.2 in the hot H_2 region as $T_{\rm ad}$ increases. The effect on emission lines of H_2 can be evaluated from one particular ratio: $\frac{1-0\ S(1)}{1-0\ S(0)}$whose integrated intensity ratio is plotted as a function of depth into the cloud on Fig. 7. One sees that this ratio is reduced by more than a factor of 3!

3.2. Influence of the radiation field

If the radiation field is increased, formation of H_2 takes place deeper into the cloud and grains are hotter. For a binding energy of $T_{\rm ad} = 800$ K, Figs. 8 and 9 show the same information as Figs. 6 and 7 for a radiation field increasing from $\chi = 10$ to $\chi = 100$.

With a higher radiation field, the point where $T_{\rm d}$ falls below $T_{\rm d}^{\rm crit}$ is pushed further and further into the cloud, as is the $\rm H/H_2$ transition. However, the later depends on screening of UV photons by self-shielding in the lines of H_2 which is more efficient than the mere effect of grains extinction. Therefore, there is a higher and higher fraction of "hot" H_2 in front of the critical point and less conversion of ortho-H_2 on grains occurs (see Fig. 2 for the position of $A_{\rm v}^{\rm c}$ as a function of $T_{\rm ad}$ for different strengths of the radiation field χ).

4. Comparison with observations

To assess the possible importance of the conversion mechanism on the interpretation of observational results, we have built a rough model of the PDR on the western edge of the ρ Ophiuchus

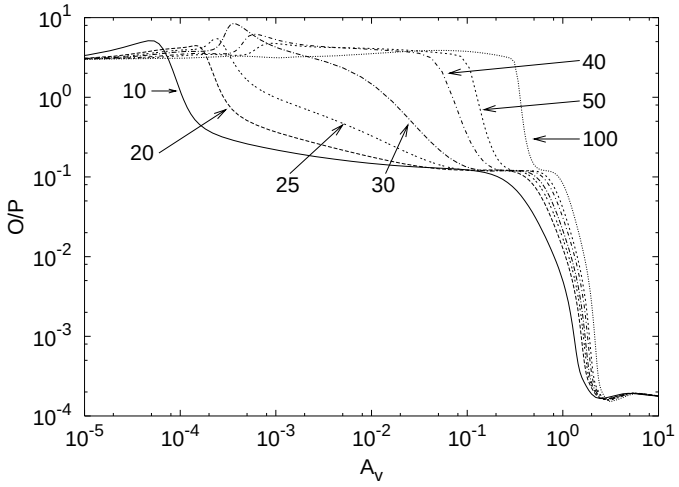

Fig. 8. O/P ratio for radiation fields increased by $\chi = 10$, 20, 25, 30, 40, 50 and 100. $T_{\rm ad} = 800$ K.

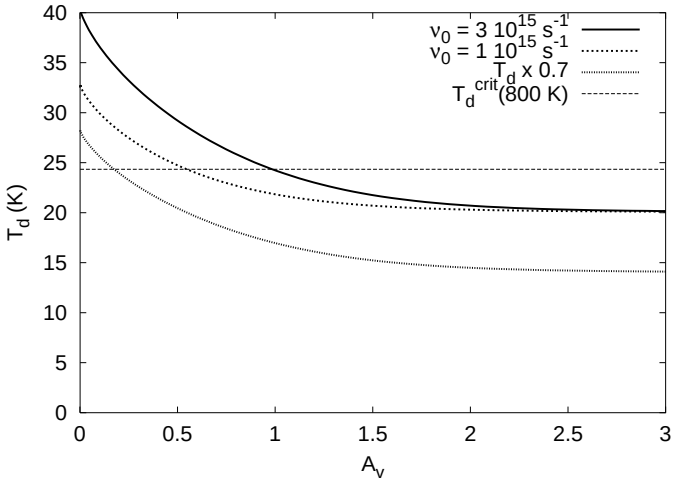

Fig. 10. Grain temperature for the HD 147889 model.

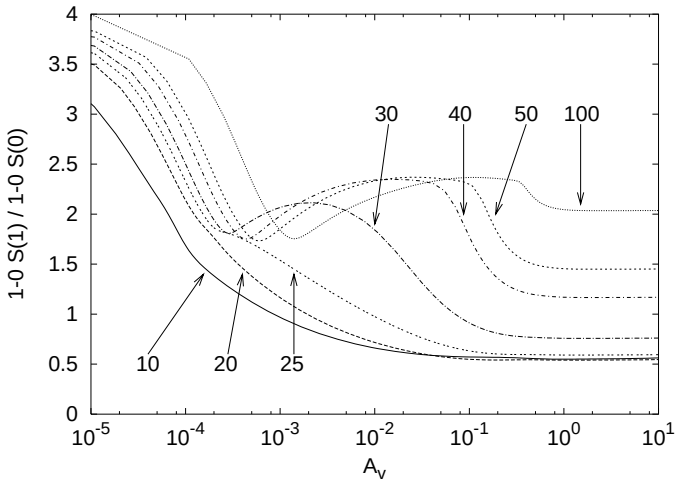

Fig. 9. Integrated intensity ratios with radiation fields of Fig. 8.

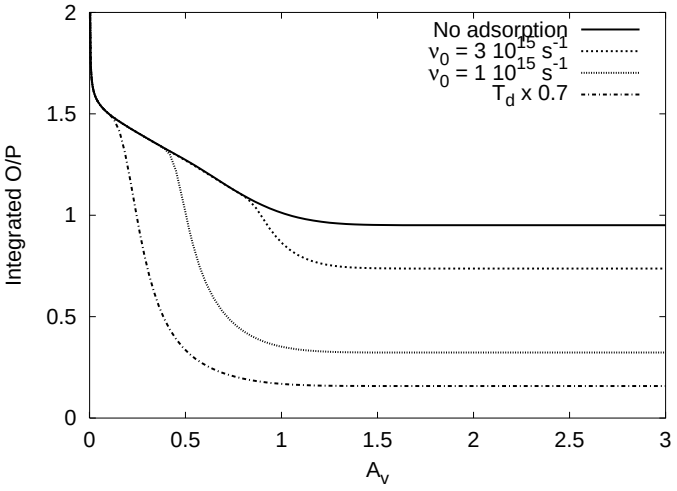

Fig. 11. Integrated O/P ratio, excluding (v=0, J=0) and (v=0, J=1).

cloud as described in Boulanger et al. (2000). We use a constant density of $n_{\rm H} = 8\,10^3\,{\rm cm}^{-3}$, a radiation field enhanced by a factor of $\chi = 300$ and a binding energy of H_2 on grains of $T_{\rm ad} = 800\,{\rm K}$. The extinction curve is that of HD 147889, and we use only small grains ($3\,10^{-7} \leq r \leq 3\,10^{-6}$ cm) to take into account the steep rise of that curve in the far UV. However, we made no further attempts to match the observations and what follows should be taken only as tendencies.

Using Eq. 1, the dust temperature at the edge is $40\,{\rm K}$, which is well above the critical dust temperature. The transition occurs around $A_{\rm v}^{\rm c} = 1$, so that the effect of our conversion mechanism is expected to be small. However, recent observations in the infra red suggest that the dust temperature may be much smaller (maybe as low as 20 K) so that it is worth exploring the consequences of different dust temperature curves. A scaling of the pre-exponential factor in Eq. 1 may be mimicked by changing ν_0. Changing ν_0 to $10^{15}\,{\rm s}^{-1}$ reduces the dust temperature to $32\,{\rm K}$ at the edge, and the transition occurs around $A_{\rm v} = 0.5$ (see Fig. 10). Alternatively, a constant scaling factor of 0.7 can be applied, resulting in a transition around $A_{\rm v} = 0.2$. In the following we present results for four models: without adsorbtion of H_2 on grains, and with adsorption using those three grain temperature curves.

Evaluating an observational O/P ratio is not an easy task. Since the information is derived from ISO observations (by nature) integrated along the line of sight and includes only emission lines, we have computed an "integrated" O/P ratio excluding the two lowest lying levels (v=0, J=0) and (v=0, J=1) of H_2 (ratio of column densities). The resulting profiles are shown in Fig. 11. Alternatively, an "observed" O/P ratio can be computed following the prescription of Wilgenbus et al. (2000), their Sect. 4. The resulting ratio, averaged over $J = 3,\ 5$ is displayed in Fig. 12.

The switching on of grain surface conversion is clearly displayed. The effect on a few selected lines is shown in Table 1 and Fig. 13. As expected, lines arising from ortho levels are reduced and lines arising from para levels are enhanced, and the effect is larger for lines emitted from deeper into the cloud (lowest rotational levels in each vibrational level).

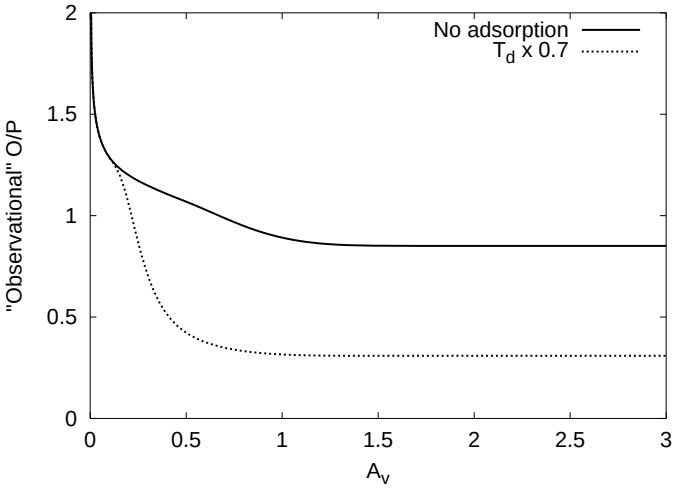

Fig. 12. "Observational" O/P ratio, following Wilgenbus et al. (2000) Sect. 4.

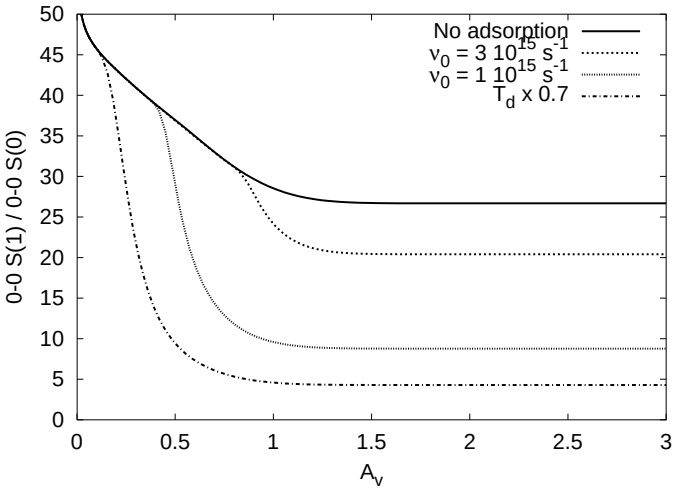

Fig. 13. Ratio of pure rotational S(0) and S(1) lines.

An excitation diagram is displayed in Fig. 14. If conversion is controlled by processing on cold grains, the rotational excitation temperature may be quite different for ortho and para H_2, as is the case here.

5. Conclusion

The O/P ratio of H_2 in PDR depends on several poorly known parameters. Here, we stress that conversion of H_2 adsorbed on grains may be fast if the grain temperature is below a threshold that depends on the binding energy of H_2 on the grain. That process could significantly affect models of PDRs, especially in regions of low radiation field. If grains are cooler in the clouds than what is computed in this model (from Hollenbach et al. (1991)), then the effect is enhanced.

Emission lines observations are difficult to use in deriving the O/P ratio. Observations in absorption from FUSE will provide direct measurements of the column densities of the lowest lying levels of H_2 in a near future, leading to much easier comparisons between models and observations.

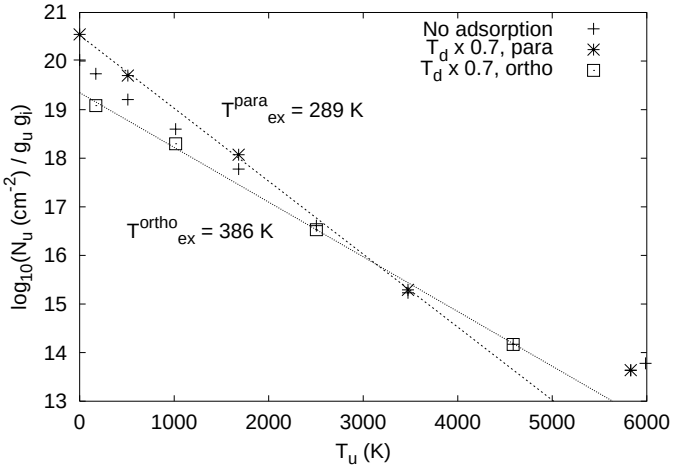

Fig. 14. Excitation diagram of the lowest levels of H_2. Column densities are computed up to $A_v = 1$.

Table 1. Selected lines emissivities (integrated up to $A_v = 10$) ($\mathrm{erg\,cm^{-2}s^{-1}sterad^{-1}}$). Numbers in parentheses are powers of 10, ν_0 is in $10^{15}\,\mathrm{s^{-1}}$.

Model	No ads.	$\nu_0 = 3$	$\nu_0 = 1$	$T_d \times 0.7$
0-0 S(0)	2.8 (-5)	3.6 (-5)	6.6 (-5)	8.6(-5)
0-0 S(1)	7.4 (-4)	7.3 (-4)	5.8 (-4)	3.7(-4)
0-0 S(2)	3.8 (-4)	3.8 (-4)	4.9 (-4)	7.6(-4)
0-0 S(3)	4.4 (-4)	4.4 (-4)	4.3 (-4)	3.6(-4)
1-0 S(0)	7.1 (-6)	7.6 (-6)	7.7 (-6)	8.7(-6)
1-0 S(1)	1.8 (-5)	1.7 (-5)	1.7 (-5)	1.6(-5)
1-0 S(2)	8.7 (-6)	8.8 (-6)	9.4 (-6)	1.0(-5)
1-0 S(3)	1.3 (-5)	1.3 (-5)	1.3 (-5)	1.2(-5)
2-1 S(1)	9.1 (-6)	9.0 (-6)	8.7 (-6)	8.0(-6)
2-1 S(2)	4.4 (-6)	4.5 (-6)	4.8 (-6)	5.4(-6)
2-1 S(3)	5.6 (-6)	5.6 (-6)	5.5 (-6)	5.1(-6)

Acknowledgements. JLB thanks E. Ilisca for pointing out that possible conversion mechanism, E. Habart for providing the extinction curve for HD 147889 and P. Goldsmith for a much needed help with the English language. As usual, I benefitted from many discussions with E. Roueff and G. Pineau des Forêts.

References

Boulanger F., Habart E., Abergel A., et al., 2000, In: ISO beyond the Peaks Conference, Madrid, ESA SP-456, in press
Buch V., Devlin J.P., 1994, ApJ 431, L135
Burton, Hollenbach D.J., Tielens A.G.G.M., 1990, ApJ 365, 620
Dissly R.W., Allen M., Anicich V.G., 1994, ApJ 435, 685
Hollenbach D.J., Takahashi T., Tielens A.G.G.M., 1991, ApJ 377, 192
Ilisca E., 1991a, J. Phys. France 1, 1785
Ilisca E., 1991b, Phys. Rev. Lett. 66, 667
Ilisca E., 1992, Prog. in Surf. Sc. 41, 213
Katz N., Furman I., Biham O., Pirronello V., Vidali G., 1999, ApJ 522, 305
Laureijs R.J., 1999, In: The Universe as seen by ISO Conference, Paris, ESA SP-427, p. 599
Le Bourlot J., 1991, A&A 242, 235
Le Bourlot J., 2000, In: ISO beyond the Peaks Conference, Madrid, ESA SP-456, in press

Le Bourlot J., Pineau des Forêts G., Roueff E., Flower D., 1995, A&A 302, 870
Palmer R.E., Willis R.F., 1987, Surf. Sc. 179, L1
Sandford S.A., Allamandola L.J., 1993, ApJ 409, L65
Tielens A.G.G.M., Allamandola L.J., 1987, In: Hollenbach D.J., Thronson H.A. (eds.) Interstellar Processes. p. 397
Wilgenbus D., Cabrit S., Pineau des Forêts G., Flower D.R., 2000, A&A 356, 1010